Compressibility effects on the Rayleigh–Taylor instability growth between immiscible fluids

D. Livescu[a)]
University of California, Los Alamos National Laboratory, Theoretical Division, T3 MS B216, Los Alamos, New Mexico 87545

(Received 28 March 2003; accepted 10 October 2003; published online 3 December 2003)

The linearized Navier–Stokes equations for a system of superposed immiscible compressible ideal fluids are analyzed. The results of the analysis reconcile the stabilizing and destabilizing effects of compressibility reported in the literature. It is shown that the growth rate n obtained for an inviscid, compressible flow in an infinite domain is bounded by the growth rates obtained for the corresponding incompressible flows with uniform and exponentially varying density. As the equilibrium pressure at the interface p_∞ increases (less compressible flow), n increases towards the uniform density result, while as the ratio of specific heats γ increases (less compressible fluid), n decreases towards the exponentially varying density incompressible flow result. This remains valid in the presence of surface tension or for viscous fluids and the validity of the results is also discussed for finite size domains. The critical wavenumber imposed by the presence of surface tension is unaffected by compressibility. However, the results show that the surface tension modifies the sensitivity of the growth rate to a differential change in γ for the lower and upper fluids. For the viscous case, the linearized equations are solved numerically for different values of p_∞ and γ. It is found that the largest differences compared with the incompressible cases are obtained at small Atwood numbers. The most unstable mode for the compressible case is also bounded by the most unstable modes corresponding to the two limiting incompressible cases. © *2004 American Institute of Physics.* [DOI: 10.1063/1.1630800]

I. INTRODUCTION

The Rayleigh–Taylor instability, which occurs due to the gravitational instability of a heavy fluid overlying a lighter fluid,[1,2] is of fundamental importance in a multitude of applications ranging from the turbulent mixing in inertial confinement fusion[3,4] to astrophysical phenomena.[5,6] Small perturbations of the interface between the two fluids grow to large amplitudes. At early times, for small enough initial perturbations, the flow can be described by the linearized equations and the amplitude grows exponentially. Later, the interface evolves into bubbles of lighter fluid and spikes of heavier fluid penetrating the opposed fluid. If the initial interface is randomly perturbed then bubbles and spikes of different sizes are generated. Mathematically, the Rayleigh–Taylor instability is an ill-posed problem and the dependence on initial conditions is still an interesting question.[7]

The theory for the linear stage for incompressible fluids agrees well with the experiments.[2,8] In the absence of surface tension and viscosity, the growth rate increases indefinitely with the wavenumber. This trend is changed by the presence of viscosity, in which case the growth rate has a peak value and decreases towards zero for large wavenumbers. On the other hand, the presence of surface tension stabilizes perturbations with the wavenumber larger than a critical value.

The role of compressibility on the development of the Rayleigh–Taylor instability between inviscid fluids has been studied by several authors,[7,9–16] however, its effect compared with the incompressible case is still under debate. The earlier studies of the linear stage dealing with ideal fluids[9,10] introduced simplifying assumptions and are strictly valid only when $\gamma=1$. Bernstein and Book[12] and Turner[16] removed these assumptions and studied the effects of compressibility as a function of γ. They found that these effects are more important at small wavenumbers and the rate of growth increases as γ decreases. They concluded that compressibility has a destabilizing effect. The same conclusion is obtained for a multilayer system by Yang and Zhang[14] by comparing the compressible growth rate with that corresponding to an incompressible system obtained as $\gamma\rightarrow\infty$. The increase in the growth rate as γ decreases can be also explained using the energy principle, as a special case of the comparison theorem in the calculus of variations.[18]

On the other hand, Sharp[7] finds a stabilizing effect of compressibility. Moreover, numerical results for late time growth seem to indicate that α (the constant of proportionality in the quadratic law for the rate of growth) increases with the speed of sound,[17] so that compressibility would have a stabilizing effect. Baker[11] found both stabilizing and destabilizing effects of compressibility in the linear regime, however, his results were based on previously derived formulas using different assumptions than ideal gas. The role of compressibility on the instability growth is thus not yet settled. Moreover, to the best of our knowledge no study of the effects of compressibility in the linear regime for viscous fluids has been performed. Additionally, there is no systematic

[a)]Electronic mail: livescu@lanl.gov

study of the effects of surface tension and finite size domain in the compressible case.

In this paper we resolve the apparent contradiction between the stabilizing and destabilizing character of compressibility for ideal fluids. We show that compressibility can be characterized by two parameters, γ and the speed of sound, with opposing influence on the instability growth. Moreover, as γ or the speed of sound (varied by changing the equilibrium pressure p_∞ at the interface while keeping the interface equilibrium density constant) increase to ∞, the limiting incompressible flows (and the bases of comparison) are different. The compressible growth rate is bounded by the growth rates obtained for these two incompressible flows which have exponentially varying and constant density, respectively.

A physical explanation for the decrease in the growth rate as p_∞ decreases can be formulated based on the influence of p_∞ on the local Atwood number. As the interface develops, the heavier fluid reaches regions of larger and larger densities of the lighter fluid while the lighter fluid reaches regions of smaller densities of the heavier fluid. The local Atwood number in these regions away from the initial position of the interface depends on p_∞, since the equilibrium density profile depends on p_∞. Using the equilibrium density provided below, it can be shown that the local Atwood number is lower for the points on the interface above the initial position, while it is higher below, compared to a system at higher p_∞ (less compressible). However, the decrease in p_∞ leads to a larger change in the local Atwood number above the initial position of the interface. The overall effect would be a decrease in the average Atwood number, thus offering an intuitive argument for the decrease of the growth rate with decreasing p_∞. Nevertheless this argument might break for small domain sizes and the validity of the results for finite size domains is discussed. The influence of surface tension and viscosity on the growth rate are also considered.

II. LINEARIZED EQUATIONS

The case of two superposed compressible ideal fluids separated by an interface at $x_1=0$ is considered. The fluids are subject to a constant gravitational acceleration $\boldsymbol{g}=(-g,0,0)$. For each fluid, the motion is governed by the continuity, momentum transport, and energy transport equations

$$\frac{\partial\rho}{\partial t}+\frac{\partial\rho u_k}{\partial x_k}=0, \tag{1}$$

$$\frac{\partial\rho u_i}{\partial t}+\frac{\partial\rho u_i u_k}{\partial x_k}=-\frac{\partial p}{\partial x_i}+\frac{\partial\tau_{ik}}{\partial x_k}-\rho g\,\delta_{i1}, \tag{2}$$

$$\frac{\partial\rho e}{\partial t}+\frac{\partial\rho e u_k}{\partial x_k}=-p\,\frac{\partial u_k}{\partial x_k}+\tau_{jk}\frac{\partial u_j}{\partial x_k}+\frac{\partial}{\partial x_k}\left(\lambda\,\frac{\partial T}{\partial x_k}\right), \tag{3}$$

where ρ is the density, u_i the velocity in x_i direction, p the pressure, e the specific internal energy, and T the temperature. The viscous stress is assumed Newtonian, $\tau_{ij}=\mu(\partial u_i/\partial x_j+\partial u_j/\partial x_i-(2/3)(\partial u_k/\partial x_k)\delta_{ij})$, and the kinematic viscosity, μ, and thermal conduction coefficient, λ, are considered constant. Equations (1)–(3) should be supplemented with equations of state for the pressure and internal energy. For each fluid, the specific heats are assumed constant, $p=R\rho T$ and $e=c_v T$, where R is the gas constant and $c_v=R/(\gamma-1)$ is the specific energy at constant volume. With these assumptions $e=p/\rho(\gamma-1)$ and the energy equation becomes

$$\frac{\partial p}{\partial t}=-\gamma p\,\frac{\partial u_k}{\partial x_k}-u_k\frac{\partial p}{\partial x_k}+(\gamma-1)\,\tau_{jk}\frac{\partial u_j}{\partial x_k}+(\gamma-1)\,\frac{\partial}{\partial x_k}\left(\lambda\,\frac{\partial T}{\partial x_k}\right). \tag{4}$$

A. Zeroth-order equations

The two fluids are assumed initially at rest and the primary variables are written as small perturbations around the equilibrium (“0”) state, with $\boldsymbol{u}\equiv 0$. Then the governing equations reduce to

$$\frac{\partial\rho_0}{\partial t}=0, \tag{5}$$

$$\frac{\partial p_0}{\partial x_1}=-\rho_0 g,\quad \frac{\partial p_0}{\partial x_2}=\frac{\partial p_0}{\partial x_3}=0, \tag{6}$$

$$\frac{\partial p_0}{\partial t}=(\gamma-1)\,\frac{\partial}{\partial x_1}\left(\lambda\,\frac{\partial T_0}{\partial x_1}\right). \tag{7}$$

Moreover, the zeroth-order variables are assumed to be in steady state, so that $\partial p_0/\partial t=0$ and T_0 and p_0 are continuous across the interface. For infinite domain or finite size domain in x_1 direction with adiabatic walls, the energy equation yields $T_0=$constant. Consequently, the equilibrium state is given by

$$\rho_{0m}=\frac{p_\infty}{R_m T_0}\exp\left(-\frac{g}{R_m T_0}x_1\right), \tag{8}$$

$$p_{0m}=p_\infty\exp\left(-\frac{g}{R_m T_0}x_1\right), \tag{9}$$

$$T_0=\text{constant}, \tag{10}$$

where p_∞ is the unperturbed pressure at the interface ($x_1=0$) and $m=1$, 2 denotes the material 1 or 2, with material 2 chosen to be above material 1.

B. First-order equations

The interface between the two fluids is perturbed with an x_2 and x_3 dependent perturbation. The location of the interface is described by the function $x_s(x_1,x_2,x_3,t)$, with $\partial x_s/\partial t=u_1$. Moreover, a surface tension is added at the interface between the two fluids. The first order linearized equations are obtained as

$$\frac{\partial\rho}{\partial t}+\rho_0\Delta+u_1 D\rho_0=0, \tag{11}$$

$$\rho_0\frac{\partial u_1}{\partial t}=-Dp-\rho g+\mu\frac{\partial}{\partial x_j}\left(\frac{\partial u_1}{\partial x_j}+Du_j\right)-\frac{2}{3}\mu D\Delta$$
$$+\sum_S T_s\left(\frac{\partial^2 x_s}{\partial x_2\partial x_2}+\frac{\partial^2 x_s}{\partial x_3\partial x_3}\right)\delta(x_1-x_s), \quad (12)$$

$$\rho_0\frac{\partial u_2}{\partial t}=-\frac{\partial p}{\partial x_2}+\mu\frac{\partial}{\partial x_j}\left(\frac{\partial u_2}{\partial x_j}+\frac{\partial u_j}{\partial x_2}\right)-\frac{2}{3}\mu\frac{\partial\Delta}{\partial x_2}, \quad (13)$$

$$\rho_0\frac{\partial u_3}{\partial t}=-\frac{\partial p}{\partial x_3}+\mu\frac{\partial}{\partial x_j}\left(\frac{\partial u_3}{\partial x_j}+\frac{\partial u_j}{\partial x_3}\right)-\frac{2}{3}\mu\frac{\partial\Delta}{\partial x_3}, \quad (14)$$

$$\frac{\partial p}{\partial t}=-\gamma p_0\Delta-u_1Dp_0+(\gamma-1)\frac{\partial}{\partial x_k}\left(\lambda\frac{\partial T}{\partial x_k}\right), \quad (15)$$

where $\Delta=\partial u_j/\partial x_j$ is the dilatation and D denotes $\partial/\partial x_1$. Equations (11)–(15) should be supplemented by boundary conditions and jump conditions across the interface. These conditions will be discussed at length in the next sections.

By examining Eqs. (11)–(15) it should be noted that in the absence of heat diffusion, the limit of incompressible flow ($\Delta=0$) can be obtained either by letting $\gamma\to\infty$ (as considered by the previous authors) or by letting $p_\infty\to\infty$ (note that since the equilibrium density at the interface should not be affected by the change in pressure, the equation of state implies $T_0\to\infty$ in this case). In the latter case the equilibrium density becomes $\rho_0=$constant, while in the former the exponential variation is still allowed. Therefore, the incompressible limit (and the base of comparison for the rate of growth) is different in the two cases. In the next sections γ and p_∞ are considered as independent parameters, both affecting the compressibility of the flow. The inviscid, infinite domain and no surface tension case will be examined first. Then the influence of finite size domain, surface tension and viscosity on the results obtained will be investigated. The nonzero heat diffusivity case was also considered, but the results were very close to the nondiffusive case and are not presented here.

III. INVISCID CASE

In general, the linearized equations do not admit analytical solutions. However, it is possible to obtain an analytical solution in the absence of viscosity and heat diffusion. Following the usual approach (e.g., Ref. 2), we seek solutions whose dependence on x_2, x_3, and time have the form

$$\exp(\boldsymbol{i}(k_2x_2+k_3x_3)+nt), \quad (16)$$

where k_2, k_3, and n are constants. For solutions having this dependence, Eqs. (11)–(15) with $\mu=0$, $\lambda=0$, become

$$n\rho=-\rho_0\Delta-u_1D\rho_0, \quad (17)$$

$$\rho_0nu_1=-Dp-g\rho-k^2T_s\delta(x_1-x_s)\frac{u_1}{n}, \quad (18)$$

$$\rho_0nu_2=-\boldsymbol{i}k_2p, \quad (19)$$

$$\rho_0nu_3=-\boldsymbol{i}k_3p, \quad (20)$$

$$np=-\gamma p_0\Delta+u_1\rho_0g, \quad (21)$$

where $\Delta=Du_1+\boldsymbol{i}(k_2u_2+k_3u_3)$ and $k^2=k_2^2+k_3^2$. After eliminating p, Δ, u_2, and u_3 from the above equations, an equation for u_1 is obtained as

$$u_1D\left[\rho_0\frac{g/c^2}{k^2+n^2/c^2}\right]-D\left[\rho_0\frac{Du_1}{k^2+n^2/c^2}\right]+\rho_0u_1$$
$$+\frac{k^2}{n^2}T_s\delta(x_1-x_s)u_1-\frac{k^2g^2}{n^2c^2}\frac{u_1}{k^2+n^2/c^2}\rho_0-u_1\frac{gD\rho_0}{n^2}$$
$$=0, \quad (22)$$

where $c=\sqrt{\gamma(p_0/\rho_0)}$ is the speed of sound. The jump condition at the interface can be obtained by integrating Eq. (22) over an infinitesimal element of x_1 which includes the interface

$$u_s\delta\left[\rho_0\frac{g/c^2}{k^2+n^2/c^2}\right]-\delta\left[\rho_0\frac{Du_1}{k^2+n^2/c^2}\right]+\frac{k^2}{n^2}T_su_s-u_s\frac{g}{n^2}\delta\rho_0$$
$$=0, \quad (23)$$

where $\delta f=f_+-f_-$, with $f_+=f(x_s+0)$, $f_-=f(x_s-0)$, is the jump of a quantity f across the interface. The subscript s denotes the value which a quantity, continuous at the interface, takes at $x_1=x_s$.

On each side of the interface, c^2 and $D\rho_0/\rho_0=-g/RT_0$ are constant, so that Eq. (22) becomes

$$D^2u_{1_m}-\frac{\gamma_mg}{c_m^2}Du_{1_m}-\left(k^2+\frac{n^2}{c_m^2}+\frac{(\gamma_m-1)g^2k^2}{n^2c_m^2}\right)u_{1_m}=0, \quad (24)$$

with the solution of the form $u_{1_m}=A_m\exp(\lambda_{1_m}x_1)+B_m\exp(\lambda_{2_m}x_1)$, where

$$\lambda_{1,2_m}=\frac{\gamma_mg}{2c_m^2}\pm k\sqrt{1+\frac{n^2}{k^2c_m^2}+\frac{(\gamma_m-1)g^2}{n^2c_m^2}+\frac{\gamma_m^2g^2}{4k^2c_m^4}}. \quad (25)$$

Formula (25) for $\lambda_{1,2_m}$ was also obtained by Amala.[15] The coefficients A_m and B_m can be determined to a multiplying constant from the conditions that u_1 vanishes at the rigid boundaries located at $x_1=-l_1$ and $x_1=l_2$ and that it is continuous over the interface. After replacing u_1 in the jump condition (23), a dispersion relation can be obtained as

$$\overline{n}^2=F_1F_2[\alpha_2\gamma_2(\gamma_1+\overline{n}^2M\alpha_1)-\alpha_1\gamma_1(\gamma_2+\overline{n}^2M\alpha_2)-\overline{T}_s(\gamma_1+\overline{n}^2M\alpha_1)(\gamma_2+\overline{n}^2M\alpha_2)]/[\alpha_1\gamma_1(\gamma_2+\overline{n}^2M\alpha_2)$$
$$\times[\overline{\lambda}_{1_1}\exp(\overline{\lambda}_{1_1}L_1)-\overline{\lambda}_{2_1}\exp(\overline{\lambda}_{2_1}L_1)]F_2-\alpha_2\gamma_2(\gamma_1+\overline{n}^2M\alpha_1)[\overline{\lambda}_{1_2}\exp(-\overline{\lambda}_{1_2}L_2)-\overline{\lambda}_{2_2}\exp(-\overline{\lambda}_{2_2}L_2)]F_1], \quad (26)$$

where the nondimensional quantities are defined as $\overline{n}^2=n^2/kg$, $M=g(\rho_1+\rho_2)/kp_\infty$, $\overline{T_s}=T_s k^2/g(\rho_1+\rho_2)$, $L_m=kl_m$, $\overline{\lambda}_{1,2_m}=\lambda_{1,2_m}/k=\alpha_m M/2\pm\sqrt{1+(1/\gamma_m)\overline{n}^2\alpha_m M+[(\gamma_m-1)/\gamma_m](\alpha_m M/\overline{n}^2)+\alpha_m^2M^2/4}$, $F_1=\exp(\overline{\lambda}_{1_1}L_1)-\exp(\overline{\lambda}_{2_1}L_1)$, and $F_2=\exp(-\overline{\lambda}_{1_2}L_2)-\exp(-\overline{\lambda}_{2_2}L_2)$. The densities $\rho_1=p_\infty/R_1T_0$ and $\rho_2=p_\infty/R_2T_0$ are the values of ρ_0 on the two sides of the interface and $\alpha_m=\rho_m/(\rho_1+\rho_2)$.

Relation (26) represents a generalization of the dispersion relations obtained by previous authors. It includes the effect of a finite size domain and surface tension, and makes no isentropic assumption. For L_1, $L_2\to\infty$ the dispersion relation becomes

$$\overline{n}^2=\frac{\alpha_2\gamma_2(\gamma_1+\overline{n}^2M\alpha_1)-\alpha_1\gamma_1(\gamma_2+\overline{n}^2M\alpha_2)-\overline{T_s}(\gamma_1+\overline{n}^2M\alpha_1)(\gamma_2+\overline{n}^2M\alpha_2)}{\alpha_1\gamma_1(\gamma_2+\overline{n}^2M\alpha_2)\overline{\lambda}_{1_1}-\alpha_2\gamma_2(\gamma_1+\overline{n}^2M\alpha_1)\overline{\lambda}_{2_2}}. \tag{27}$$

As explained above, the incompressible flow limit ($\Delta=0$) can be obtained either by letting $p_\infty\to\infty$ or $\gamma\to\infty$. As $p_\infty\to\infty$, the flow approaches incompressible flow with constant density, for which the nondimensional rate of growth is given by

$$\overline{n'}_i^2=\frac{\alpha_2-\alpha_1-\overline{T_s}}{\alpha_1\coth(L_1)+\alpha_2\coth(L_2)}, \tag{28}$$

which for infinite domain becomes $\overline{n'}_i^2=\alpha_2-\alpha_1-\overline{T_s}$.[2] On the other hand, as $\gamma\to\infty$, the equilibrium flow has still exponentially varying density, with the dispersion relation

$$\begin{aligned}\overline{n''}_i^2=&F_1F_2[\alpha_2-\alpha_1-\overline{T_s}]/\\&[\alpha_1[\overline{\lambda^i}_{1_1}\exp(\overline{\lambda^i}_{1_1}L_1)-\overline{\lambda^i}_{2_1}\exp(\overline{\lambda^i}_{2_1}L_1)]F_2^i\\&-\alpha_2[\overline{\lambda^i}_{1_2}\exp(-\overline{\lambda^i}_{1_2}L_2)\\&-\overline{\lambda^i}_{2_2}\exp(-\overline{\lambda^i}_{2_2}L_2)]F_1^i]F_1^iF_2^i,\end{aligned} \tag{29}$$

where $\overline{\lambda^i}_{1,2_m}=\alpha_mM/2\pm\sqrt{1+\alpha_mM/\overline{n''}_i^2+\alpha_m^2M^2/4}$ and F_m^i are defined using $\overline{\lambda^i}_{1,2_m}$. The parameter M is related to the exponent in the formula for the unperturbed density $\rho_{0_m}=\rho_m\exp(-M\alpha_m kx_1)$. For infinite domain and no surface tension Eq. (29) reduces to the formula derived by Bernstein and Book[12]

$$\overline{n''}_i^2=-M\alpha_1\alpha_2+\sqrt{M^2\alpha_1^2\alpha_2^2+(\alpha_2-\alpha_1)^2} \tag{30}$$

and it is easy to show that $\overline{n''}_i^2<\overline{n'}_i^2$ for $M>0$ and $\overline{n''}_i^2\to\overline{n'}_i^2$ as $M\to0$.

In the dispersion formula for the compressible case [Eq. (26)] the decrease in p_∞ is equivalent to an increase in M at γ constant. Thus, for the compressible case, M represents a measure of the compressibility effects on the rate of growth. On the other hand, M is proportional to the ratio between the wavelength of the initial perturbation and the density exponential change length scale. For small values of M, this lengthscale is much larger than the wavelength of the initial perturbation, and the rate of growth approaches the incompressible, constant density result.

For infinite domain, an approximate relation for $\overline{n}^2$, valid to order $O(M)$ for small values of M is

$$\begin{aligned}\overline{n}^2\approx\overline{n'}_i^2\Bigg[&1+M\left[\left(\frac{\alpha_1}{\gamma_1}-\frac{\alpha_2}{\gamma_2}\right)\alpha_1\alpha_2-\frac{\overline{T_s}}{2}\left(\frac{\alpha_1^2}{\gamma_1}+\frac{\alpha_2^2}{\gamma_2}\right)\right]\\&+M\alpha_1\alpha_2\left(\frac{1}{\gamma_1}-\frac{1}{\gamma_2}\right)-\frac{M}{2}\left(\frac{\gamma_1-1}{\gamma_1}\alpha_1^2-\frac{\gamma_2-1}{\gamma_2}\alpha_2^2\right)\Bigg]\\&-\frac{M}{2}\left(\frac{\gamma_1-1}{\gamma_1}\alpha_1^2+\frac{\gamma_2-1}{\gamma_2}\alpha_2^2\right).\end{aligned} \tag{31}$$

For $\gamma_1=\gamma_2=1$ the relation derived by Plesset and Prosperetti[10] is recovered. In general, for γ_1, $\gamma_2\geqslant1$, it can be shown that relation (31) implies $\overline{n}^2<\overline{n'}_i^2$ for any combination of parameters, with the constraint $\rho_2>\rho_1$. Moreover, Fig. 1 shows that $\overline{n}^2$ decreases as p_∞ decreases. It should be noted that the same effects of decreasing p_∞ on the nondimensional growth rate can be obtained either by increasing g or decreasing k, with all other parameters kept constant. In other words, compressibility effects are more important at larger values of g and lower wavenumbers, which is supported by the numerical solutions of the dispersion relation presented in Fig. 1.

For large M and no surface tension, it follows from the dispersion relation that

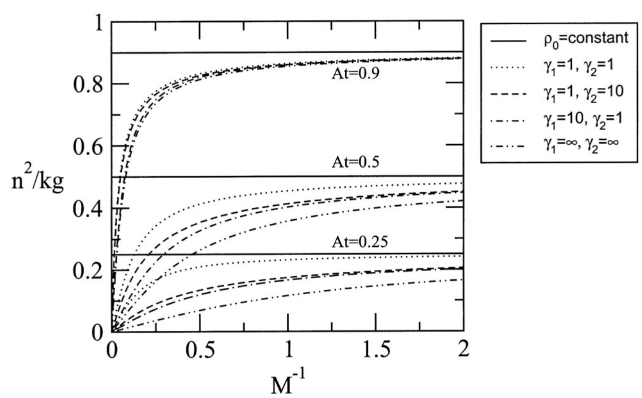

FIG. 1. Nondimensional rate of growth as function of $1/M=kp_\infty/g(\rho_1+\rho_2)$ for different values of γ_1 and γ_2.

$$\overline{n}^2 \approx \frac{1}{M} \frac{(\alpha_2-\alpha_1)^2}{\alpha_1\alpha_2\left(\alpha_1\frac{\gamma_2-1}{\gamma_2}+\alpha_2\frac{\gamma_1-1}{\gamma_1}+\sqrt{\alpha_1^2+\alpha_2^2+2\frac{\gamma_1\gamma_2-2\gamma_1-2\gamma_2+2}{\gamma_1\gamma_2}\alpha_1\alpha_2}\right)}. \tag{32}$$

A further reduction in the rate of growth can be obtained by increasing the adiabatic exponents. At the limit, when γ_1, $\gamma_2 \to \infty$, the nondimensional rate of growth becomes

$$\overline{n}^2 \approx \frac{1}{M} \frac{(\alpha_2-\alpha_1)^2}{2}, \tag{33}$$

which is the same as that obtained from formula (30) for large M by Bernstein and Book[12] and Turner.[16] In general, for finite values of M it can be shown[12,16] that increasing the ratio of specific heats leads to a decrease in the rate of growth, also supported by Fig. 1. However, the rate of growth has different sensitivities to the change of γ_1 and γ_2. Thus, as Fig. 1 shows, the change in the ratio of specific heats of the lower fluid leads to a larger change of n. Therefore, the rate of growth is more sensitive to the change in compressibility of the lower fluid. Moreover, as Fig. 1 indicates, these results are also sensitive to the value of the Atwood number. For large values of the Atwood number the results obtained for the compressible cases show little sensitivity to changes in the ratios of specific heats and the rate of growth obtained for the compressible case is close to the incompressible variable density result. Nevertheless, at small Atwood numbers and for large M, the values of γ_1 and γ_2 become important in determining the rate of growth. In addition, the relative difference between the growth rates obtained for the two limiting incompressible flows increases as the Atwood number decreases, so that compressibility effects are larger at small Atwood numbers.

In conclusion, the instability growth rate for a compressible flow (n) in the inviscid, infinite domain and no surface tension case is bounded by the growth rates of the corresponding incompressible flows obtained for uniform (n_i') and exponentially varying density (n_i''), so that $n_i'' < n < n_i'$. As p_∞ increases (so that the flow becomes less compressible), n increases towards n_i', while as γ increases (so that the fluid becomes less compressible), n decreases toward n_i''.

A. Influence of finite size domain

For the case in which the domain is bounded by rigid boundaries located at $x=-l_1$ and $x=l_2$, the growth rates obtained for constant density incompressible flow and incompressible flow with exponentially varying density are given by Eqs. (28) and (29), respectively. Figure 2(a) presents the growth rate as a function of the nondimensional parameter M for different domain sizes. For domain sizes not very small compared to the wavelength of the perturbation, the nondimensional growth rate is still bounded by $\overline{n_i'}$ and $\overline{n_i''}$ and the rate of growth decreases as the domain size decreases. However, similar to the incompressible case, the decrease in $\overline{n}$ is less significant when L_1 is decreased. Therefore, for $L_1 < L_2$ the growth rate varies more when p_∞ is changed, so it is more sensitive to the change in compressibility.

For the extreme case when $L_2 \ll 1$ (domain size small compared to the wavelength of the initial perturbation) and $\gamma_1 \approx 1$ it is possible, as Fig. 2(b) shows, that the compressible growth rate becomes larger than the constant density incompressible growth rate for M smaller than a critical value. Numerical solutions of the dispersion relation (26) for a large range of parameters indicate that the curve $\overline{n}^2$ can intersect only once the line $\overline{n}^2 = \overline{n'}_i^2$. Therefore, an analytical condition for the existence of the overshoot can be found by letting $M \to 0$ (in which case the dispersion relation simplifies considerably) and imposing $\overline{n}^2 > \overline{n'}_i^2$. After some algebra one obtains

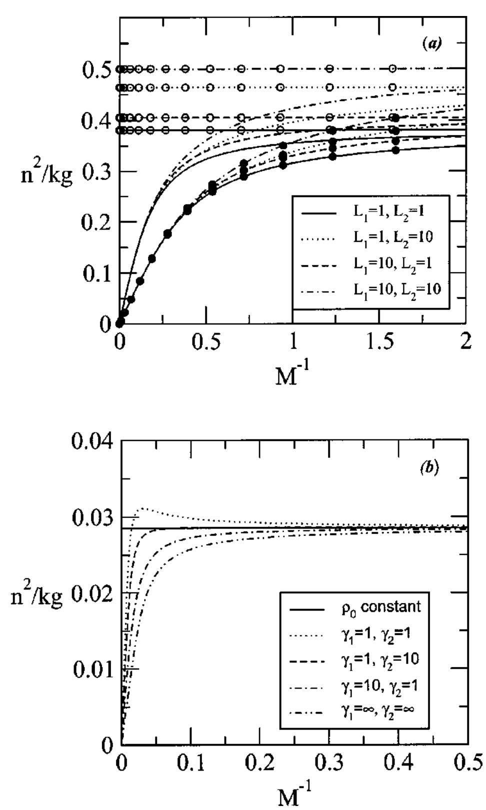

FIG. 2. Finite size effect on the nondimensional rate of growth. (a) No symbols curves represent the compressible case with $\gamma_1=\gamma_2=1.4$, open symbols the corresponding constant density incompressible case and closed symbols the corresponding variable density incompressible case. (b) $L_1=0.1$, $L_2=0.05$. All cases have At=0.5.

$$\frac{\alpha_1 \coth L1+\alpha_2 \coth L_2}{2}\left[\frac{\gamma_1-1}{\gamma_1}\frac{\alpha_1^2}{\overline{n'}_i^2}\Phi_1+At+2\alpha_1\alpha_2 \times\left(\frac{\alpha_1}{\gamma_1}-\frac{\alpha_2}{\gamma_2}\right)\frac{\coth L_1+\coth L_2}{\alpha_1\coth L1+\alpha_2\coth L_2}+\frac{\gamma_2-1}{\gamma_2}\frac{\alpha_2^2}{\overline{n'}_i^2}\Phi_2\right] +\frac{At}{2}\left(\frac{\alpha_1^2}{\gamma_1}\Phi_1+\frac{\alpha_2^2}{\gamma_2}\Phi_2\right)>0, \tag{34}$$

where $\Phi_m=L_m\coth^2 L_m-\coth L_m-L_m$ varies from 0 to -1 as L_m increases from 0 to ∞. Consistent with the numerical results, condition (34) can be fulfilled only for small values of the domain size of the upper fluid and ratio of specific heats close to 1 for the lower fluid.

B. Influence of surface tension

The presence of surface tension tends to inhibit the growth of the instability. Moreover, for the incompressible case there is a critical wavenumber $k_c=[(\rho_2-\rho_1)g/T]^{1/2}$,[2] so that the arrangement is stable for $k>k_c$. By imposing $n=0$ in the dispersion relation (26) it can be seen that the critical wavenumber remains the same as in the incompressible case. However, for $T_s\neq 0$, the wavenumber appears as an explicit parameter in the dispersion relation (26) so the variations of p_∞ and k are no longer equivalent. Nevertheless, at each k, the nondimensional compressible rate of growth obtained for infinite domain is still bounded by $\overline{n'}_i^2$ and $\overline{n''}_i^2$, as Fig. 3 shows. However, the lower limit is approached differently as γ_1 or γ_2 increase to ∞. Thus, the variation in the compressibility of the lower fluid is more important at lower wavenumbers, while the variation in the compressibility of the upper fluid is more important at higher wavenumbers.

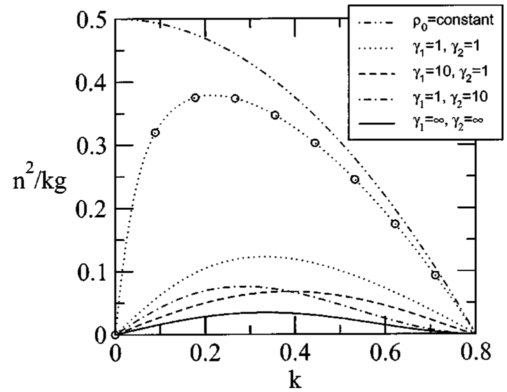

FIG. 3. Compressibility influence on the nondimensional rate of growth in the presence of surface tension, for $T_s/g(\rho_1+\rho_2)=0.78\ \mathrm{m}^2$. All compressible cases have $g(\rho_1+\rho_2)/p_\infty=4\ \mathrm{m}^{-1}$ except the open symbol case for which $g(\rho_1+\rho_2)/p_\infty=0.4\ \mathrm{m}^{-1}$.

IV. EFFECT OF VISCOSITY

Consider the case of two viscous fluids, bounded by two rigid surfaces at $x=-l_1$ and $x=l_2$. Following the previous procedure, the linearized equations can be reduced to a single fourth order ordinary differential equation in u_1 of the form

$$A_4D^4u_1+A_3D^3u_1+A_2D^2u_1+A_1Du_1+A_0u_1=0, \tag{35}$$

where the coefficients A_i are given in the Appendix for the compressible case and the two incompressible limiting cases. However, only for the uniform density incompressible case this equation has constant coefficients and an easily derived analytical solution. The boundary conditions for Eq. (35) are $u_i=0$ at $x=-l_1$ and $x=l_2$, u_i and tangential viscous stresses continuous at the interface, and a jump condition found from the integration of the governing equation over the interface. For the compressible case, the condition that tangential velocities vanish at the rigid boundary can be written as $\Delta-Du_1=0$ at $x=-l_1$ and $x=l_2$, while the continuity of u_2 and u_3 at the interface leads to the continuity of $\Delta-Du_1$. The divergence of the velocity fluctuations is given by

$$\Delta=B_3D^3u_1+B_2D^2u_1+B_1Du_1+B_0u_1, \tag{36}$$

with the coefficients B_i given in the Appendix. The continuity of the tangential viscous stress over the interface can be written as

$$\delta(\mu[D\Delta-D^2u_1-k^2u_1])=0. \tag{37}$$

An expression for $D\Delta$ in terms of the derivatives of u_1 is provided in the Appendix. The jump condition at the interface can be found by eliminating p, u_2, and u_3 from the momentum equation and integrating the resulting equation over an infinitesimal element of x_1 which includes the interface

$$\delta\left[\left(-\rho+\frac{\mu}{n}D^2\right)(\Delta-Du_1)\right]+\frac{k^2}{n}\delta(\mu Du_1) =-\frac{k^2}{n^2}[g(\rho_2-\rho_1)-k^2T_s]u_s -\frac{2k^2}{n}(\mu_2-\mu_1)(\Delta-Du_1)_s. \tag{38}$$

For $\Delta=0$ condition (38) reduces to the condition derived for the incompressible case in Ref. 2. In the Appendix an expression for $D^2\Delta$ is provided. Since u_1 can be found only to a multiplying constant, the boundary conditions are supplemented with the specification of u_1 or one of its derivatives at one point inside the domain. Then Eq. (35) together with the boundary conditions described above form a closed set of equations from which u_1 on each side of the interface and the rate of growth n can be determined. For all cases considered l_1 and l_2 are large compared to the wavelength of the initial perturbation so the configuration is close to the infinite domain case. Equation (35) was integrated on each side of the domain using a fourth order Runge–Kutta scheme. In order to determine n and u_1 from the matching conditions at the interface, a multidimensional secant method (Broyden's method) was employed.

Figure 4 presents numerical solutions of the viscous linearized equations for different Atwood numbers. Consistent with the previous results, the compressible rate of growth is bounded by the incompressible rates of growth obtained for uniform density and exponentially varying density cases.

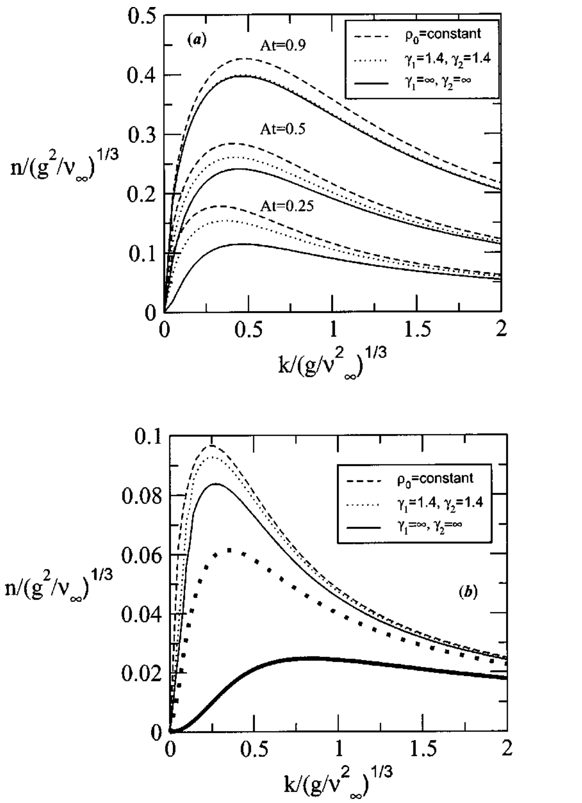

FIG. 4. Growth rate dependency on the wavenumber for viscous fluids. (a) The compressible and incompressible variable density cases have $M=0.1$. (b) At$=0.1$, compressible and variable density incompressible cases showed with thick lines correspond to $M=0.1$ and with thin lines to $M=0.01$.

Moreover, its behavior is similar to the well known incompressible constant density result. It has a peak at some critical wavenumber and decreases towards zero as the wavenumber becomes large. However, the location of the peak is different compared to the incompressible case, with the highest difference at small Atwood numbers. Here we should note a qualitative difference between the results obtained for the constant density incompressible case and those obtained for the compressible and variable density incompressible cases. At small Atwood numbers, the critical wavenumber decreases with Atwood number for the constant density incompressible case, while it increases for the other two cases. Moreover, as shown in the previous sections, the largest differences in the inviscid rate of growth compared to the constant density incompressible case are obtained at small wavenumbers and small Atwood numbers. It is expected then that, for the viscous case at small Atwood numbers, the relative difference between the rate of growth obtained for the compressible and incompressible cases considered will be largest, also confirmed by Figs. 4(a) and 4(b). Although this difference should become very small as M approaches zero, Fig. 4(b) shows that, for small Atwood numbers, it persists at smaller values of M.

V. CONCLUSIONS

The effects of compressibility on the growth rate of Rayleigh–Taylor instability between two immiscible ideal fluids are examined in the linear regime. The results distinguish between the stabilizing and destabilizing character of compressibility. For infinite domains, the growth rate n obtained for the compressible case is bounded by the growth rates obtained for the corresponding incompressible flows with constant and exponentially varying density, and this result is not affected by the presence of surface tension or viscosity. For ideal gases with zero heat diffusivity, the limiting incompressible flow (defined by $\partial u_i/\partial x_i=0$) can be attained either by increasing the ratio of specific heats, γ, or the speed of sound (varied by changing the equilibrium pressure at the interface at constant equilibrium density at the interface). The equilibrium density distribution for the limiting incompressible flow is different in the two cases. Moreover, the two parameters have opposing influence on the rate of growth. As the speed of sound is increased, the rate of growth increases towards the value obtained for the corresponding constant density incompressible flow, while as γ increases, n decreases towards the value obtained for the corresponding incompressible flow with exponentially varying density. The presence of heat diffusion was also considered, but the results were very close to those obtained for the nondiffusive case and were not presented here.

The equilibrium density for a compressible flow varies exponentially with x_1 and depends on p_∞. Therefore, the local Atwood number changes as the interface moves away from the original position. Compared to a flow with a higher value of p_∞ (less compressible), the local Atwood number decreases for the points on the interface situated above the initial position, while it increases for the points on the interface situated below the initial position. However, the change in the local Atwood number is larger above the initial position of the interface, so that the overall effect would be a decrease of the average local Atwood number. This offers an intuitive argument for the decrease of the growth rate as p_∞ decreases. Moreover, this argument suggests that the bubble velocity decreases, while the spike velocity increases for more compressible flows. On the other hand, as γ decreases the fluids are more compressible, however the equilibrium density and pressure do not change. Therefore, as the heavier fluid moves towards regions of higher pressures, its volume decreases and the volume change is larger for more compressible fluids, so that the spike velocity decreases. Similarly, for more compressible fluids the bubble velocity increases. If the two fluids have different values for γ, it is shown that the growth rate is more sensitive to the change in the ratio of the specific heats of the lower fluid. However, at large Atwood numbers the rate of growth is little influenced by the values of γ_1 and γ_2 and p_∞ becomes the main compressibility parameter. In addition, it is shown that compressibility effects are more important at small Atwood numbers.

For domains bounded by rigid surfaces, the compressible growth rate is still bounded by the two incompressible growth rates described above, except for the extreme case when the domain size of the upper fluid is small compared to the wavelength of the initial perturbation and $\gamma\approx 1$ for the lower fluid. In this case, the compressible growth rate can become larger than the growth rate obtained for the corresponding constant density incompressible flow for values of the compressibility parameter $M=(g(\rho_1+\rho_2))/kp_\infty$ smaller than a critical value. An analytical condition for the existence of this overshoot is provided. In general, the results show that the compressible growth rate varies more when the rigid boundary of the lower fluid is closer to the interface than the rigid boundary of the upper fluid, so that it is more sensitive to the change in compressibility.

The presence of surface tension tends to inhibit the growth rate of the instability and for the incompressible case there is a critical wavenumber above which the configuration becomes stable. It is shown that the value of this critical wavenumber is not affected by compressibility. For wavenumbers below this critical value the general result presented above remains valid. However, the presence of surface tension modifies the sensitivity of the growth rate to a differential change in the value of γ for the two fluids. At smaller wavenumbers, the change in γ for the lower fluid is more important for the variation of n, while the opposite holds true at higher wavenumbers.

Numerical solutions of the linearized equations show that for viscous compressible fluids, the growth rate behaves in a manner analogous to the incompressible growth rate. It has a most unstable wavenumber and decreases towards zero at larger wavenumbers. Moreover, both the growth rate and the most unstable mode are bounded by the values obtained for the corresponding constant and variable density incompressible flows. For the constant density incompressible flow it is known that the most unstable mode moves to small wavenumbers as the Atwood number is decreased. The inviscid results presented in this paper show that the effects of compressibility are more important at small wavenumbers and small Atwood numbers. Consistent with these results, it is found that for viscous fluids compressibility becomes more important at small Atwood numbers. For small enough Atwood numbers, the difference between the compressible and incompressible growth rates will remain sizable at larger values of the equilibrium pressure.

An interesting question raised by the results presented in this paper is if they remain valid in the nonlinear regime for single and/or multimode initial perturbation. Our preliminary numerical results seem to indicate a similar influence of p_∞ and γ on the growth rate (and on the spike and bubble velocities) to that found in the linear regime. Moreover, even for large values of the equilibrium pressure so that the early time results are close to the incompressible flow results, the late time spike and bubble velocities become different than in the incompressible case. Another interesting question is about the range of the amplitudes of the perturbation for which the growth rate agrees with the linear theory prediction. Again, our preliminary numerical results seem to indicate that the range of validity of the linear assumption remains approximately the same as in the incompressible case. These results will be published elsewhere.

This study was concerned with the effects of compressibility on the instability growth between immiscible fluids with uniform equilibrium temperature. It does not cover many of the configurations of practical interest, for example the presence of an equilibrium temperature gradient, a more general equation of state or diffuse interfaces, which might be important in certain applications.[3,19] However this study offers a systematic approach for examining the effects of compressibility which could represent a starting point for analyzing different or more complex configurations.

ACKNOWLEDGMENTS

The author would like to thank Dr. Timothy T. Clark and Dr. Francis H. Harlow for their advice on the preparation of this article and many helpful and insightful discussions. Computational resources were provided through the Institutional Computing Project, Los Alamos National Laboratory. This work was supported by the U.S. Department of Energy.

APPENDIX: EQUATIONS FOR THE VISCOUS CASE

Following the usual procedure for the incompressible, constant density case, the variables are nondimensionalized using $1/n_0=(g^2/\nu_\infty)^{-1/3}$ as time scale and $1/k_0=(g/\nu_\infty^2)^{-1/3}$ as lengthscale. The compressibility parameter M is defined by $M=g(\rho_1+\rho_2)/k_0 p_\infty$. For simplicity the kinematic viscous coefficient is considered continuous over the interface, so that $\mu_1/\rho_1=\mu_2/\rho_2$, with μ_1 and μ_2 constant on each side of the interface. The value of the kinematic viscous coefficient at the interface is denoted by ν_∞.

The scaled equations for u_1 and Δ on each side of the interface can be written as

$$A_4 D^4 u_1 + A_3 D^3 u_1 + A_2 D^2 u_1 + A_1 D u_1 + A_0 u_1 = 0, \quad \text{(A1)}$$

$$\beta_1 \Delta = B_3 D^3 u_1 + B_2 D^2 u_1 + B_1 D u_1 + B_0, \quad \text{(A2)}$$

where the coefficients (with the index m denoting the side of the interface suppressed for simplicity) are given by

$$A_4 = B_3 \beta_1 \beta_2, \quad \text{(A3)}$$

$$A_3 = (DB_3 + B_2)\beta_1\beta_2 - B_3\omega, \quad \text{(A4)}$$

$$A_2 = (DB_2 + B_1)\beta_1\beta_2 + \exp(\alpha M x)\beta_1^2 - B_2\omega, \quad \text{(A5)}$$

$$A_1 = (DB_1 + B_0)\beta_1\beta_2 - \frac{\beta_1^2}{n} - B_1\omega, \quad \text{(A6)}$$

$$A_0 = DB_0\beta_1\beta_2 - (n + k^2\exp(\alpha M x))\beta_1^2 - B_0\omega, \quad \text{(A7)}$$

$$B_3 = \frac{\exp(\alpha M x)}{\beta_2}\left(\gamma + \frac{4}{3}\beta_3\right), \quad \text{(A8)}$$

$$B_2 = -\frac{\alpha M \exp(\alpha M x)}{\beta_2^3}\left[\gamma - \left(2\gamma - \frac{4}{3}\right)\beta_3\right], \quad \text{(A9)}$$

$$B_1 = -\frac{n}{\beta_2^2}\left[\frac{\alpha^2 M^2 \exp(\alpha M x)}{n}\left(\gamma - 1 - \frac{1}{3}\beta_3\right) + \beta_2\left(\gamma + \frac{4}{3}\beta_3\right)\left(1 + \frac{k^2}{n}\exp(\alpha M x)\right)\right], \quad \text{(A10)}$$

$$B_0 = -\frac{\alpha n M}{\beta_2^2}\left[\beta_3\left(\gamma - 1 - \frac{1}{3}\beta_3\right) + (2\gamma - 1)\alpha M k^2 \exp(\alpha M x) + \frac{M k^2 \beta_2}{\alpha n^2}\right], \quad \text{(A11)}$$

$$DB_3=\frac{\gamma\alpha^2M^2n\exp(2\alpha Mx)}{\beta_2^2}, \tag{A12}$$

$$DB_2=\frac{\alpha^3m^3n\exp(2\alpha Mx)}{3\beta_2^3}\left(7\gamma-3-\frac{6\gamma-4}{3}\beta_3\right), \tag{A13}$$

$$DB_1=\frac{\alpha Mn}{\beta_2^3}\left[\alpha^3m^3\exp(2\alpha Mx)\left(3\gamma-2-\frac{1}{3}\beta_3\right)+\beta_3^2\beta_2\left(\frac{1}{3}-\gamma\frac{k^2}{\alpha Mn^2}\right)+\beta_2^3\right], \tag{A14}$$

$$DB_0=\frac{\alpha^2M^2n}{\beta_2^3}\left[\frac{\alpha^2M^2\exp(2\alpha Mx)}{n}(\gamma-1)^2\left(\gamma-1-\frac{1}{3}\beta_3\right)-(2\gamma-1)\alpha Mk^2\exp(2\alpha Mx)\left(\gamma-\frac{1}{3}\beta_3\right)+\frac{k^2}{\alpha Mn^2}\beta_2^3\right], \tag{A15}$$

$$\beta_1=\frac{n}{\beta_2^2}\left[\frac{\alpha^2M^2\exp(\alpha Mx)}{n}(\gamma-1)\left(\gamma-1-\frac{1}{3}\beta_3\right)-\beta_2^2\left(1+\gamma\frac{Mk^2}{\alpha n^2}+\frac{4k^2}{3n}\exp(\alpha Mx)\right)\right], \tag{A16}$$

$$\beta_2=\gamma+\tfrac{1}{3}\beta_3, \tag{A17}$$

$$\beta_3=\alpha Mn\exp(\alpha Mx). \tag{A18}$$

The equation for $D\Delta$ can be written as

$$D\Delta=\frac{\alpha Mn}{\beta_2}\left[\frac{\gamma-1}{n}\Delta-\exp(\alpha Mx)D^2u_1+\frac{1}{n}Du_1+(n+k^2\exp(\alpha Mx))u_1\right], \tag{A19}$$

while the equation for $D^2\Delta$ is

$$D^2\Delta=\frac{\alpha Mn}{\beta_2}\left[\frac{\alpha M(\gamma-1)}{n\beta_2}\left(\gamma-1-\frac{1}{3}\beta_3\right)\Delta-\exp(\alpha Mx)D^3u_1+\left(\frac{1}{n}-\frac{(2\gamma-1)M\exp(\alpha Mx)}{\beta_2}\right)D^2u_1\right.$$
$$\left.+\left(\frac{\alpha M}{n\beta_2}\left(\gamma-1-\frac{1}{3}\beta_3\right)+n+k^2\exp(\alpha Mx)\right)Du_1+\left(\frac{\alpha Mn}{\beta_2}\left(\gamma-1-\frac{1}{3}\beta_3\right)+\frac{(2\gamma-1)\alpha Mk^2\exp(\alpha Mx)}{n\beta_2}\right)u_1\right]. \tag{A20}$$

For $\gamma\to\infty$ or $p_\infty\to\infty\,(M\to 0)$, Eqs. (A2), (A19), and (A20) yield $\Delta=0$, $D\Delta=0$, and $D^2\Delta=0$, so the incompressible case is recovered. In the case $\gamma=\infty$ the equation for u_1 simplifies to

$$D^4u_1-(n\exp(-\alpha Mx)+2k^2)D^2u_1+n\alpha M\exp(-\alpha Mx)Du_1+\left(n\exp(-\alpha Mx)+\frac{\alpha M}{n}\exp(-\alpha Mx)+k^2\right)k^2u_1=0. \tag{A21}$$

If, furthermore, $M\to 0$ in Eq. (A21), then the well-known equation for uniform density incompressible fluid derived in Ref. 2 is obtained. The same equation can be obtained by letting $p_\infty\to\infty\,(M\to 0)$ directly in Eq. (A1).

[1] G. I. Taylor, ''Instability of liquid surfaces when accelerated in a direction perpendicular to their planes,'' Proc. R. Soc. London, Ser. A **201**, 192 (1950).
[2] S. Chandrasekhar, *Hydrodynamic and Hydromagnetic Stability* (Dover, New York, 1981).
[3] J. D. Kilkenny, S. G. Glendinning, S. W. Haan, B. A. Hammel, J. D. Lindl, D. Munro, B. A. Remington, S. V. Weber, J. P. Knauer, and C. P. Verdon, ''A review of the ablative stabilization of the Rayleigh–Taylor instability in regimes relevant to inertial confinement fusion,'' Phys. Plasmas **1**, 1379 (1994).
[4] J. P. Knauer, R. Betti, D. K. Bradley, T. R. Boehly, T. J. B. Collins, V. N. Goncharov, P. W. McKenty, D. D. Meyerhofer, V. A. Smalyuk, C. P. Verdon, S. G. Glendinning, D. H. Kalantar, and R. G. Watt, ''Single-mode Rayleigh–Taylor growth-rate measurements on the OMEGA laser system,'' Phys. Plasmas **7**, 338 (2000).
[5] B. A. Remington, S. V. Weber, M. M. Marinak, S. W. Haan, J. K. Kilkenny, R. J. Wallace, and G. Dimonte, ''Single-mode and multimode Rayleigh–Taylor experiments on Nova,'' Phys. Plasmas **2**, 241 (1995).
[6] D. R. Farley and L. M. Logory, ''Single-mode, nonlinear mix experiments at high Mach number using Nova,'' Astrophys. J., Suppl. Ser. **127**, 311 (2000).
[7] D. H. Sharp, ''An overview of Rayleigh–Taylor instability,'' Physica D **12**, 3 (1984).
[8] J. T. Wadell, C. E. Niederhaus, and J. W. Jacobs, ''Experimental study of Rayleigh–Taylor instability: Low Atwood number liquid systems with single-mode initial perturbation,'' Phys. Fluids **13**, 1263 (2001).
[9] P. O. Vandervoort, ''The character of the equilibrium of a compressible, inviscid fluid of varying density,'' Astrophys. J. **134**, 699 (1961).
[10] M. S. Plesset and A. Prosperetti, ''Reply to comments on 'General analysis of the stability of superposed fluids','' Phys. Fluids **25**, 911 (1982).
[11] L. Baker, ''Compressible Rayleigh–Taylor instability,'' Phys. Fluids **26**, 950 (1983).
[12] I. B. Bernstein and D. L. Book, ''Effect of compressibility on the Rayleigh–Taylor instability,'' Phys. Fluids **26**, 453 (1983).
[13] A. M. Lezzi and A. Prosperetti, ''Rayleigh–Taylor instability for adiabatically stratified fluids,'' Phys. Fluids A **1**, 1784 (1989).

[14]Y. Yang and Q. Zhang, ''General properties of a multilayer stratified fluids system,'' Phys. Fluids A **5**, 1167 (1993).
[15]P. Amala, ''Large-eddy simulation of the Rayleigh–Taylor instability on a massively parallel computer,'' Lawrence Livermore National Laboratory Report UCRL-LR-119748 (1995).
[16]L. Turner, ''Rayleigh–Taylor instabilities and gravity waves in compressible fluids,'' Los Alamos National Laboratory Report LA-UR-02-6439 (2002).
[17]X. L. Li, ''Study of three-dimensional Rayleigh–Taylor instability in compressible fluids through level set method and parallel computation,'' Phys. Fluids A **5**, 1904 (1993).
[18]W. A. Newcomb, ''Compressibility effects on instability growth rates,'' Phys. Fluids **26**, 3246 (1983).
[19]R. E. Duff, F. H. Harlow, and C. H. Hirt, ''Effects of diffusion on interface instability between gases,'' Phys. Fluids **5**, 417 (1962).